

Small-signal response of a laser to cavity-length modulation: A diagnostic for dynamical models and parameter values

J. Y. Gao, H. Z. Zhang, X. Z. Guo, and G. X. Jin

Department of Physics, Jilin University, Changchun, Jilin, People's Republic of China

N. B. Abraham*

*Laboratoire de Spectroscopie Hertzienne, Université Sciences et Techniques de Lille, Flandres Artois,
Bâtiment P5, F-59655 Villeneuve d'Ascq, CEDEX, France*

(Received 15 May 1989)

We consider the small-signal response of a rate-equation laser to modulation of the laser cavity length. To avoid nonlinear resonances in modulators and power supplies, we demonstrate that one can hold the modulation frequency and amplitude fixed while varying the cavity detuning to change the resonant response of the laser to modulation, and thereby one can extract the relaxation oscillation frequency and the damping rate of those oscillations. This technique permits a careful study of the relaxation parameters of the laser that govern small oscillations and thereby permits discrimination among several different models recently proposed to describe CO₂ laser dynamics. We demonstrate this method of analysis by applying it to such a laser experimentally with the result that the simple rate-equation model is shown to fail while the more complex vibro-rotational model satisfactorily describes the results.

INTRODUCTION

Ever since it was noted that lasers using ruby, yttrium aluminum garnet (YAG), CO₂, and semiconductors as the gain medium displayed damped relaxation oscillation transients following sudden changes in the excitation or laser cavity loss, modulation of a parameter has been used to generate giant "Q-switched" pulses at rates slightly less than the relaxation oscillation frequency.¹ It is readily found that the modulation need not be 100% of the difference between the unsaturated gain and loss (thereby actively turning the laser off once each cycle), but that for many lasers only a few percent modulation is sufficient to generate distortions from sinusoidal response often in the form of trains of giant pulses separated by intervals of nearly zero intensity.²

The sensitive dependence of these lasers to modulation and the weakly damped relaxation oscillation transients can be viewed in two ways. In the point of view of the behavior of the standard Maxwell-Bloch equations or laser-Lorenz equations for a single-mode laser interacting with a two-level, homogeneously broadened medium, these characteristics arise from a particular relationship among the decay rates for the field, polarization, and population variables. The typical lasers designed with the materials mentioned above are lasers for which the polarization can be adiabatically eliminated, yielding equations for the field amplitude and the population inversion. Furthermore, these are lasers for which the field decay rate is much more rapid than the population-inversion decay rate. The weakly damped transients reflect the existence of a pair of complex-conjugate eigenvalues governing the stability of the lasing solution that have negative real parts that are much smaller in magni-

tude than the imaginary parts.

Laser media that are accurately described as two-level, homogeneously broadened materials are few, but many can be effectively described this way. This is because the behavior of much more complex models (involving individual populations of many levels and many interlevel polarizations) can often be reduced to dynamics in a particular two-dimensional subspace of the phase space which can then be effectively described by two coupled equations for motion in that subspace. This is formally accomplished by the center-manifold theory. The strong response to modulation and the weakly damped transients are indications that the dynamics in this manifold are those of a weakly damped oscillator. Using this more general approach a much wider range of lasers can be described by a generic class of two coupled equations.

Such lasers are often discussed as a class because of their similar behavior, though the particular values of the decay rates determine the corresponding frequencies and damping rates of the damped oscillations. This group of lasers was first identified in the selective adiabatic eliminations in the studies by Tang^{3(a)} of the simple laser model and in a classification scheme in the Russian literature [Belenov *et al.* and Genkin and Khanin, Ref. 3(b)] and has more recently been popularized for the study of lasers dynamics as "class-B" lasers.⁴

The nonlinear response of a CO₂ laser to modulation was used by Arecchi and co-workers in one of the earliest studies of optical chaos.⁵ Further experiments have been performed with cavity-loss modulation,⁶ gain modulation,⁷⁻⁸ and cavity-length modulation⁹ in CO₂ lasers, primarily for the study of nonlinear dynamics (period doublings, chaos, crises, etc.). Other class-B lasers have been studied for relaxation oscillations transients under step-

wise excitation and for their nonlinear dynamics under sinusoidal modulation.¹⁰ Theoretical studies have explored the sequence of nonlinear modulation resonances¹¹ as a function of modulation strength and frequency and many of these results have been observed recently in an analog simulation of the equations.¹² The details of the nonlinear resonances and the families of coexisting periodic and chaotic oscillations and their collisions and crises have been found in numerical simulations and linked to the relative degrees of conservative and dissipative character in the dynamics.¹³

It was demonstrated in Ref. 7 that such lasers are much more sensitive to loss modulation than pump modulation when the modulation frequency is close to the relaxation oscillation frequency. This relative sensitivity has been observed experimentally (see discussion in Ref. 7) and the analysis of Ref. 7 has been extended to the case of cavity-length modulation.¹⁴ No experiments on the linear-dynamical response of a CO₂ laser to length modulation as a function of cavity detuning have been reported previously, but the nonlinear dynamics have been shown to be sensitive (with evidence of period doublings, chaos, and crises) to cavity detuning under either length modulation⁹ or gain modulation.⁸

The response of the class-*B* lasers to loss modulation can be so strong that it is relatively difficult to have a sinusoidal response to sinusoidal modulation unless the modulation amplitude is extremely weak. This is because the damped resonance is characterized by a Toda potential¹⁵ which is highly anharmonic for all but the smallest oscillations and because the relatively weak damping in these lasers usually permits excitation of large excursions. Nevertheless, we propose to explore the small-signal response regime because of its utility in confirming the parameters of the damped relaxation oscillator. Such explorations might equally well be carried out with loss or gain modulation, which also show resonances. However, both CO₂ and YAG lasers can have their relaxation oscillation resonances (of the order of 30–300 kHz) inconveniently near the characteristic frequencies of mechanical resonances in piezoelectric, acousto-optic, or electro-optic modulators. Such resonances limit the tuning range of the modulators and make it difficult to monitor the actual modulation amplitude as a function of modulation frequency. We thus take the approach of modulating the cavity length at a fixed frequency and tuning the parameters of the damped relaxation oscillator of the laser by changing the laser cavity detuning.

There are several different ways of extracting the characteristics of the small-signal response in terms of the real and imaginary parts of the eigenvalues governing the stability of the steady-state laser solution. One can use a stepwise change in the excitation to obtain a damped relaxation oscillation, and from the oscillation frequency and the decay of the amplitude of the oscillations one can extract the laser parameters.^{10(a), 10(c), 10(f)} The alternative route is to evaluate the resonant response of the system to weak periodic modulation. In its simplest form this method entails measuring the response as a function of the modulation frequency (for fixed modulation amplitude); the width and center frequency of the

resonance peak can be used to extract the real and imaginary parts of the eigenvalues. For reasons discussed above we pursue a variation of this method in order to characterize the resonance features.

These studies have special current merit because of the debate that has recently appeared over the necessary and sufficient models for the description of the dynamics of a CO₂ laser. Many studies have used a simple two-level, rate-equation model^{4–14, 16} even though the population dynamics in a CO₂ laser is known to involve complicated couplings of many vibrational and rotational levels. However, careful analysis of the multilevel models reveals that most populations have rapid decay rates and that the population decays are limited by a pressure-dependent bottleneck in the decay of the lower vibrational manifold (that includes the lower laser level) to the ground state. This permits adiabatic elimination of the fast levels (including the laser levels) leaving the dynamics of the population inversion between the upper and lower vibrational manifolds which contain the actual lasing sublevels (001-10⁰). The result is that one arrives effectively to the same rate equations for a population inversion and the field that one would have by simply adiabatically eliminating the polarization in the standard two-level, homogeneously broadened atom model. However, this has been shown to be inadequate to describe the dynamics of CO₂ lasers with saturable absorbers^{15, 17, 18} (LSA) and CO₂ lasers with switched parameters.¹⁹ The explanation is that the sum of the upper and lower populations in a CO₂ laser does not remain constant (as is necessarily required for validity of a two-level model). In the latter case it was proposed to return to a more complex model originally proposed for CO₂ lasers²⁰ in which the intravibrational band relaxation of the rotational levels is proposed to play a key dynamical role. This model also formed the basis of the LSA studies in Refs. 15 and 18.

It may seem surprising that there would be any debate over the models for such a well-known and well-used laser as the CO₂ Refs. 21 and 22, but this is a reflection of the relatively recent emergence of the nonlinear-dynamical studies. In the theoretical modeling of nonlinear dynamics, most authors are content to use the simplest model that explains the observed experimental results rather than using the extremely complicated models developed for the explanation of efficiencies and *Q*-switching characteristics. This is because most physical results depend primarily on the existence of a damped resonance (such as that in the two-level model) and thus they are frequently not sensitive to model-dependent subtleties except insofar as they change the parameters of the damped resonance.^{5, 6, 9–13} That the details of exact dynamical models for CO₂ lasers are still uncertain is evident from the continuing discussion and measurements.^{15, 17–19, 23–25}

From the nonlinear-dynamical point of view there are now at least three physically distinct models: the simple two-level picture for which one uses equations only for the intensity and the population difference of the two vibrational manifolds; a three-level picture requiring two separate equations for the upper- and lower-level populations;¹⁷ and the intraband relaxation model requiring

population difference equations both for the two levels involved in the lasing emission and for the two vibrational bands.^{15,18–20} The latter model has been simplified by the center-manifold technique to an equivalent two-equation system.²⁴ This contrasts with a multiple-time-scale analysis^{19,25} using more traditional methods of adiabatic elimination which leads to a similar, though less exact, result.

Each of these models predicts damped oscillations with the resonant frequency and the damping rate dependent on the different physical parameters. In the case of the simple laser with a two-level medium these parameters are simply the degree of excitation above the lasing threshold, the cavity detuning measured in units of the polarization decay rate, the field decay rate and the population inversion decay rate. As these quantities can be determined independently in a straightforward manner, it is possible to compare their values to the characteristics of the relaxation oscillations. The relationships between the decay parameters and the oscillations will add credence to the claims that the more complex models are necessary. While this has been demonstrated in the nonlinear dynamics, the studies we propose will show that such complex models are needed even to describe the response to slight modulation of the laser about its steady-state values. In particular, the model with interband relaxation processes predicts damping rates for the relaxation oscillations that are as much as twenty times greater than are found in the two-level model while the frequency of the oscillations is relatively unchanged.

SMALL-SIGNAL RESPONSE TO MODULATION

To illustrate the effects of detuning on the response to modulation we consider the two-level model, beginning with the basic laser rate equations including cavity detuning. We assume that all changes are slow compared with the polarization decay rate permitting adiabatic elimination of the polarization amplitude. We further assume that the laser frequency adiabatically follows changes in the cavity length. (This development parallels that given in Refs. 7 and 14, but as important subtleties are to be exploited in our fitting of experimental data, we expand upon the results found in Ref. 14.) Then

$$\frac{dD}{dt} = -\gamma_{\parallel}[D - 1 + ID/(1 + \delta^2)], \quad (1a)$$

$$\frac{dI}{dt} = -2\kappa I[1 - AD/(1 + \delta^2)], \quad (1b)$$

$$\delta = (\omega_C - \omega_A)/\gamma_{\perp}[1 + (\kappa/\gamma_{\perp})], \quad (1c)$$

where D and I are the suitably normalized variables for the population difference and the laser intensity, respectively, with their respective decay rates γ_{\parallel} and 2κ (we retain κ as the decay rate of the electric field in the laser cavity); A is the laser pump rate normalized to unity at the laser threshold for a resonant cavity; and δ is the detuning of the laser frequency from the center of the two-level resonance in units of the decay rate of the polarization. δ is expressed in the usual mode-pulling formula in terms of the laser cavity frequency and the material reso-

nance frequency in Eq. (1c).

The steady-state nontrivial solution is given by

$$I_{SS} = A - 1 - \delta_0^2, \quad (2a)$$

$$D_{SS} = (1 + \delta_0^2)/A. \quad (2b)$$

Linearizing about this solution we find that the eigenvalues of the linear stability analysis are given by

$$\lambda = -(\gamma_{\parallel} A'/2) \pm i[2\kappa\gamma_{\parallel}(A' - 1) - (\gamma_{\parallel} A'/2)^2]^{1/2}, \quad (3)$$

where $A' = A/(1 + \delta_0^2)$. It is clear that $\text{Re } \lambda$ is always negative indicating that the steady state is stable. If $\kappa \gg \gamma_{\parallel}$, we see that the decay rate is slow compared with the oscillations which are given approximately by the frequency ω_0

$$|\text{Im } \lambda| \approx \omega_0 \equiv [2\kappa\gamma_{\parallel}(A' - 1)]^{1/2}. \quad (4a)$$

We also define the value of ω_0 for $\delta_0 = 0$ given by

$$\omega_{0_{\text{max}}} \equiv [2\kappa\gamma_{\parallel}(A - 1)]^{1/2}. \quad (4b)$$

For a typical low-pressure CO₂ lasers (at about 10 Torr), κ is of order 10^7 s^{-1} while γ_{\parallel} is of order $5 \times 10^4 \text{ s}^{-1}$, governed primarily by the pressure. For a laser a few times above threshold, we show in Fig. 1 the variation of steady-state intensity, the eigenvalue $\text{Im } \lambda$, and ω_0 as functions of detuning.

The response of this system to modulation of the cavity length is given by considering the addition of a modulated cavity length as specified by

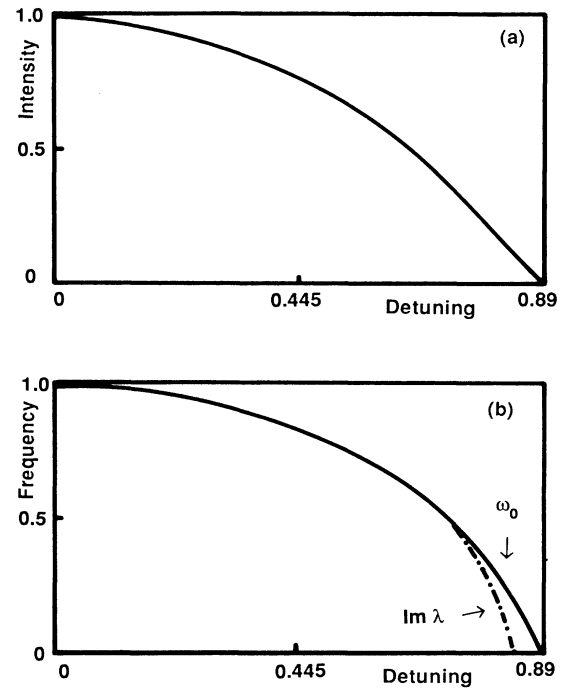


FIG. 1. Plot of steady-state solutions and their characteristics for the two-level model from Eqs. (2)–(4) using $A = 1.8$, $\kappa = 1 \times 10^7 \text{ s}^{-1}$, $\gamma_{\parallel} = 6 \times 10^4 \text{ s}^{-1}$. (a) I_{SS} vs δ_0 ; (b) ω_0 (solid line) and $\text{Im } \lambda$ (dotted line shows where it deviates from ω_0). Intensity and frequencies are normalized to unity at zero detuning.

$$\frac{dD}{dt} = -\gamma_{\parallel} [D - 1 + ID / (1 + \delta^2)] , \quad (5a)$$

$$\frac{dI}{dt} = -2\kappa I [1 - AD / (1 + \delta^2)] , \quad (5b)$$

$$\delta = \delta_0 + m \cos \Omega t . \quad (5c)$$

For a small modulation depth and $\delta_0 \gg m$ we can use the approximation

$$(1 + \delta^2)^{-1} \approx (1 + \delta_0^2)^{-1} \{ 1 - [2\delta_0 m \cos(\Omega t)] / (1 + \delta_0^2) \} , \quad (6a)$$

and linearizing about the steady-state solution by writing

$$I = I_{SS} + a , \quad (6b)$$

$$D = D_{SS} + b , \quad (6c)$$

we arrive at the equation for the amplitude of the intensity modulation

$$\frac{d^2 a}{dt^2} + \beta \frac{da}{dt} + \omega_0^2 a = F \cos(\Omega t + \phi + \pi) , \quad (7a)$$

where

$$F = 4\kappa \delta_0 m (A' - 1) (\gamma_{\parallel}^2 + \Omega^2)^{1/2} , \quad (7b)$$

$$\tan \phi = -(\Omega / \gamma_{\parallel}) , \quad (7c)$$

$$\beta = \gamma_{\parallel} A' . \quad (7d)$$

As was done for ω_0 , we call the line-center value of β , β_{\max}

$$\beta_{\max} \equiv \gamma_{\parallel} A . \quad (7e)$$

We have made a variety of assumptions of adiabatic following in the course of this derivation, and while these are the traditional arguments, one may doubt their validity if one is to make a careful comparison between theoretical predictions and experimental results. The formal justification can be found in Ref. 26 where the center-manifold technique has been applied to the five equations for the interaction of a single mode with a two-level medium in the presence of detuning. They demonstrate explicitly that when $\kappa \gg \gamma_{\parallel}$, the dynamics in the vicinity of the steady-state solutions can be described by motion on a two-dimensional submanifold with a damped resonance of exactly the sort described above.

It is of interest to note the difference with the vibrational-rotational model developed in Refs. 15 and 20 where an equivalent damped oscillator equation is found²⁴ with changes in the parameters given by

$$\beta \rightarrow \gamma_{\parallel} [A' + (A' - 1)J\kappa / (J + 1)\gamma_R] , \quad (8a)$$

$$\omega_0^2 \rightarrow 2\kappa \gamma_{\parallel} (A' - 1) \text{ (unchanged)} , \quad (8b)$$

where γ_R is the intraband relaxation rate and J is the number of rotational levels involved in the intraband relaxation. Clearly β does not depend sensitively on J for values of $J \geq 10$, and as this number has recently been proposed to be as large as 15–20 for the *P*20 line (see

Refs. 19, 24, 25, 27, and 28) it may be difficult to infer anything about its value. (Recent cross-spectral saturation measurements would suggest, however, that J may be only of the order of 4–5.²³ In contrast, the rotational-relaxation rate to all other levels in the vibrational manifold $(J + 1)\gamma_R$ at pressures above 10 Torr should involve the same mechanisms as the polarization decay rate γ_{\perp} and thus these rates should be equal in the equivalent two-level model.

The amplitude of response a_0 as given by solutions to Eqs. (8) in the form

$$a(t) = a_0 \cos(\Omega t + \phi + \pi + \Theta) \quad (9)$$

is expressed as

$$a_0 = 4\kappa \delta_0 m (A' - 1) (\gamma_{\parallel}^2 + \Omega^2)^{1/2} \times [(\omega_0^2 - \Omega^2)^2 + 4\beta^2 \Omega^2]^{-1/2} . \quad (10)$$

It is helpful to rewrite Eq. (10) as

$$a_0 = C y_1(\delta_0) y_2(\delta_0) , \quad (11a)$$

where

$$C = 4\kappa m , \quad (11b)$$

$$y_1(\delta_0) = \delta_0 (A' - 1) = \delta_0 [A - (1 + \delta_0^2)] / (1 + \delta_0^2) = I_{SS}(\delta_0) [\delta_0 / (1 + \delta_0^2)] , \quad (11c)$$

$$y_2(\delta_0) = (\gamma_{\parallel}^2 + \Omega^2)^{1/2} [(\omega_0^2 - \Omega^2)^2 + 4\beta^2 \Omega^2]^{-1/2} . \quad (11d)$$

Physically $y_1(\delta_0)$ corresponds to the product of the slope of the intensity versus detuning curve ($2\delta_0$) (which is an “adiabatic” factor giving the amplitude of the steady-state intensity modulation corresponding to adiabatic following of the frequency modulation) and the normalized degree above threshold at that detuning ($A' - 1$). The second factor $y_2(\delta_0)$ is the resonant response of the damped resonance of the system to modulation at frequency Ω when the resonance of the system has eigenvalues given by $\lambda = -(\beta/2) \pm i[\omega_0^2 - (\beta/2)^2]^{1/2}$. This result appears in Ref. 14 though the full range of variation (particularly for $\Omega > \omega_{0\max}$) and its applicability for fitting experimental results was not explored.

Figures 2(a)–2(c) show the functions $a_0(\delta_0)$, $y_1(\delta_0)$, and $y_2(\delta_0)$ normalized to their peak values for cases in which Ω is less than $\omega_{0\max}$. Figure 2(d) shows an example for $\Omega > \omega_{0\max}$. Figure 3 summarizes the characteristics of such curves. Figure 3(a) shows the value of δ_0 that gives the peak of $a_0(\delta_0)$ for different values of Ω and a second curve on the same graph shows the value of ω_0 for each value of δ_0 . Figure 3(b) shows the actual (unnormalized) height of the maximum value of $a_0(\delta_0)$ as a function of Ω . Figure 4 shows how the dashed curve in Fig. 3(a) depends on the parameters for fixed value of their product (fixed relaxation oscillation frequency). Figure 5 gives the half-width at half-maximum of the curves for $a_0(\delta_0)$ in Fig. 2.

From Fig. 2 we infer the following trends.

(a) For a fixed modulation frequency Ω , $a_0(\delta_0)$ has a peak as δ_0 is scanned.

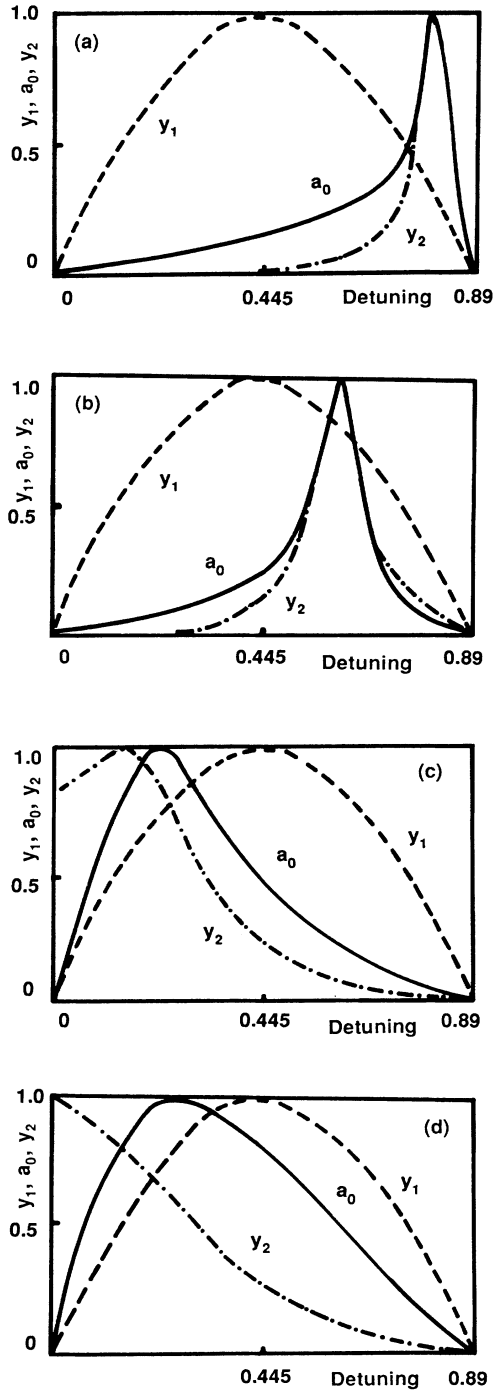


FIG. 2. Plot of functions identified in Eq. (11) for $A=1.8$, $\kappa=1 \times 10^7 \text{ s}^{-1}$, $\gamma_{\parallel}=6 \times 10^4 \text{ s}^{-1}$; $a_0(\delta_0)$ (solid line), $y_1(\delta_0)$ (dashed line), $y_2(\delta_0)$ (dot-dashed line). Values of Ω (angular frequency) are (a) $3 \times 10^5 \text{ s}^{-1}$; (b) $6 \times 10^5 \text{ s}^{-1}$; (c) $9.5 \times 10^5 \text{ s}^{-1}$; (d) $11 \times 10^5 \text{ s}^{-1}$.

(b) For small values of Ω (less than $\omega_{0_{\max}}$) the curve $a_0(\delta_0)$ is governed primarily by the curve $y_2(\delta_0)$, the resonance peak is very narrow and occurs for relatively large detuning. At the resonance, $\Omega = \text{Im}\lambda$.

(c) For larger values of Ω the peak in $a_0(\delta_0)$ moves

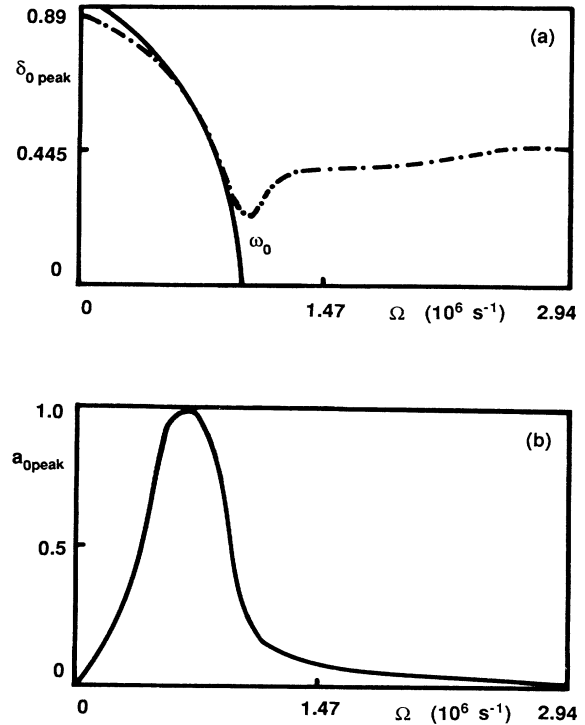


FIG. 3. Plot of the characteristics of the peak in $a_0(\delta_0)$ [(a) defining $\delta_{0 \text{ peak}}$ and (b) $a_{0 \text{ peak}}$] for $A=1.8$, $\kappa=1 \times 10^7 \text{ s}^{-1}$, $\gamma_{\parallel}=6 \times 10^4 \text{ s}^{-1}$ as functions of Ω . For comparison, the value of ω_0 for the steady-state solution specified by $\delta_0 = \delta_{0 \text{ peak}}$ is plotted as a solid line in (a).

closer to line center (smaller values of detuning) and the peak becomes wider.

(d) When Ω is greater than $\omega_{0_{\max}}$, the peak moves to larger values of δ_0 and the curve $a_0(\delta_0)$ approaches the function $y_1(\delta_0)$.

We summarize the results in Figs. 3–5 as follows.

(i) When $\Omega \gg \omega_{0_{\max}}$ the resonance peak appears at an asymptotic value of the detuning given by

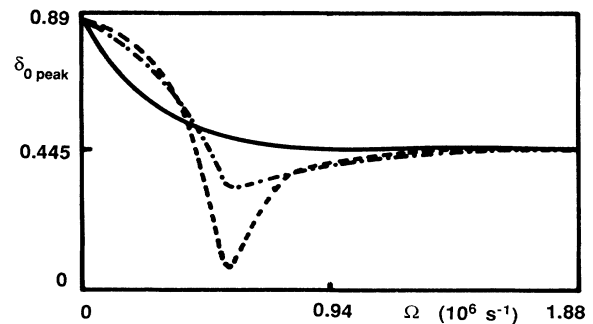


FIG. 4. For comparison with the dotted curve in Fig. 3(a) with $A=1.8$ and $\kappa\gamma_{\parallel}=2 \times 10^{11} \text{ s}^{-2}$ but different parameters $\kappa=2 \times 10^8 \text{ s}^{-1}$, $\gamma_{\parallel}=1 \times 10^3 \text{ s}^{-1}$ (dashed curve); $\kappa=2.5 \times 10^6 \text{ s}^{-1}$, $\gamma_{\parallel}=8.0 \times 10^4 \text{ s}^{-1}$ (dot-dashed curve); $\kappa=4.4 \times 10^5 \text{ s}^{-1}$, $\gamma_{\parallel}=4.5 \times 10^5 \text{ s}^{-1}$ (solid line).

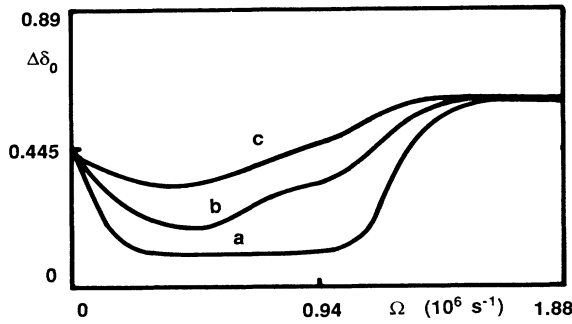


FIG. 5. This figure gives the half-width at half-maximum ($\equiv \Delta\delta_0$) of the curve $a_0(\delta_0)$ as a function of Ω for $\kappa\gamma_{\parallel} = 8.75 \times 10^{11} \text{ s}^{-1}$ but different parameters (a) $\kappa = 8.75 \times 10^8 \text{ s}^{-1}$, $\gamma_{\parallel} = 1 \times 10^3 \text{ s}^{-1}$; (b) $\kappa = 5.83 \times 10^6 \text{ s}^{-1}$, $\gamma_{\parallel} = 1.5 \times 10^5 \text{ s}^{-1}$ (c) $\kappa = 3.5 \times 10^6 \text{ s}^{-1}$, $\gamma_{\parallel} = 2.5 \times 10^5 \text{ s}^{-1}$.

$\delta'_0 = \left\{ \frac{1}{2} [(A^2 + 8A)^{1/2} - (A + 2)] \right\}^{1/2}$, which is the maximum of $y_1(\delta_0)$, and the width of the resonance approaches the width of the curve $y_1(\delta_0)$.

(ii) The convergence of the curves for ω_0 and Ω in a certain range in Fig. 3(a) indicates that the resonance in the output corresponds to matching of the modulation frequency to the internal relaxation frequency.

(iii) When Ω is much larger than $\omega_{0\text{max}}$ we see that the peak in the resonant response of the system is simply given by the location of the maximum slope in the intensity as a function of detuning since the resonance condition cannot be achieved for any detuning.

(iv) When for large detuning the laser is taken close to threshold, the curves again diverge showing that the approximate formula ω_0 used for $\text{Im}\lambda$ is no longer correct.

(v) Figure 3(b) shows the peak of the $a_0(\delta_0)$ curve as a function of the modulation frequency. The maximum occurs at the frequency for which $y_1(\delta_0)$ and $y_2(\delta_0)$ have their peaks at the same detuning.

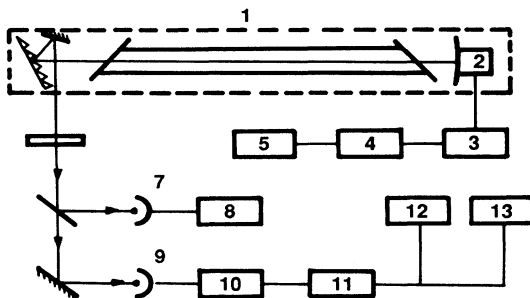


FIG. 6. Schematic of the experimental setup. (1) Single-mode tunable CO₂ laser; (2) piezoelectric ceramic (PZT) used for cavity-length modulation; (3) dc power supply for δ_0 tuning; (4) amplifier; (5) signal generator; (6) attenuator; (7) pyroelectric detector; (8) galvanometer; (9) HgCdTe detector; (10) preamplifier; (11) frequency selective amplifier; (12) oscilloscope; (13) high-frequency voltmeter.

From the convergence of the curves in Fig. 3 for small Ω we see that one can use the experimental values for the resonance peak for δ_0 in order to estimate the value of $\omega_{0\text{max}}$. From the width of the resonances in δ_0 compared with Fig. 5 (when $\Omega < \omega_{0\text{max}}$) one can also determine β . β also governs the divergence of the curves in Fig. 3(a) at high values of Ω . Knowing β_{max} and $\omega_{0\text{max}}$ (which permits a prediction of the values of κ and γ_{\parallel} depending on the particular model), the measured values can be used to determine which of the various dynamical models discussed earlier gives values consistent with direct measurements or estimates of these decay rates.

EXPERIMENTAL RESULTS

Figure 6 shows our CO₂ laser experimental setup and Fig. 7 shows the resonance curves $a_0(\delta_0)$ as in Fig. 2. Figures 8(a) and 8(b) show the summary corresponding to Figs. 3(a), 4, and 5; Fig. 9 for reference shows the average intensity output for each detuning. We note that there is a small shoulder on the curve in Fig. 9 which we interpret as the presence of a weak transverse mode (as it did not appear on the negative detuning side) and hence we disregard data for detunings larger than 1.24.

The limit of 300 kHz for Ω was given by the end of the response range of the piezoelectric ceramic on which the mirror was mounted. We note that by following the resonance in δ_0 , we are not sensitive to the resonances in the PZT which often distort attempts to follow $a_0(\Omega)$ for fixed δ_0 . By normalizing each curve $a_0(\delta_0)$ to its maximum we need only follow the location of the peak and the width of the peak to extract the desired information.

Our laser was operated on the P36 line of CO₂ with a wavelength of 10.76 μm . The power at line center was about 1 W for a total gas pressure of 17 Torr with a mixture of gases Xe:CO₂:N₂:He of 1.00:2.22:3.50:17.00. The discharge was dc excited at a current of 11 mA. The laser discharge length was 80 cm and the laser cavity length was 115 cm giving a sufficiently large free spectral range so that we obtained single-mode operation. An aperture was placed in the cavity to suppress unwanted transverse modes. From the estimated window and mirror losses for the field (taken to be 12% per roundtrip) we expect a cavity decay rate of

$$\kappa \equiv -c \ln(1-l)/2L = (1.7 \pm 0.3) \times 10^7 \text{ s}^{-1},$$

where L is the length of the laser, and l is the losses.

CHARACTERISTICS OF CO₂ 10.6 μm TRANSITIONS

The rotational relaxation rate $(J+1)\gamma_R$ for our pressures can be determined from the data of Cheo's²² Table 18:

$$[(1.1 \pm 0.2)P_{\text{CO}_2} + (1.0 \pm 0.2)P_{\text{N}_2} + (0.7 \pm 0.1)P_{\text{He}}] \times 10^7 \text{ s}^{-1} \text{ Torr}^{-1}.$$

Using this formula gives a value of $(1.4 \pm 0.3) \times 10^8 \text{ s}^{-1}$

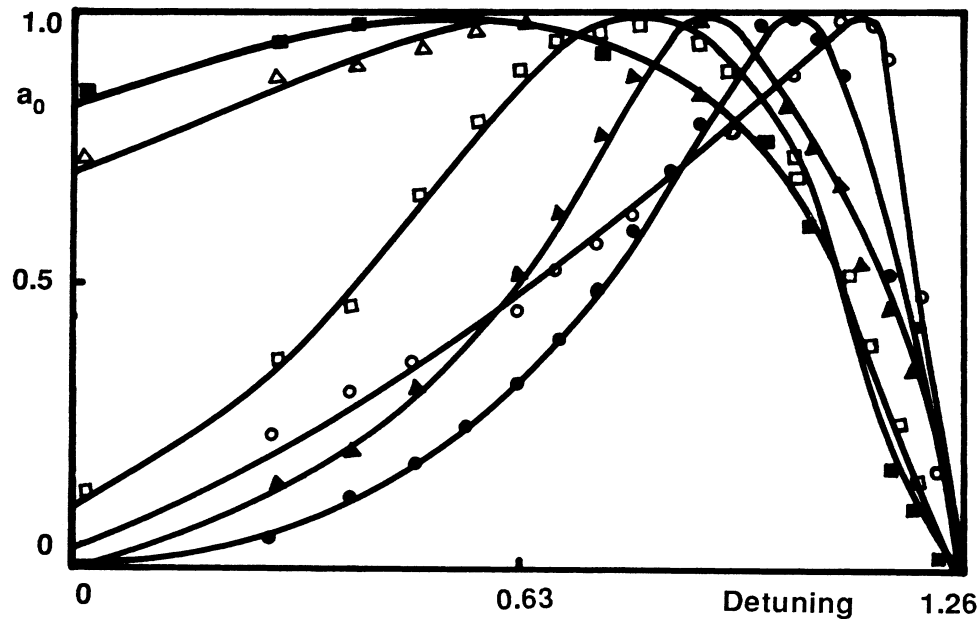


FIG. 7. Experimental results for $a_0(\delta_0)$ at different values of Ω . Solid curves smoothly connect each set of data. Values of Ω (angular frequency) are open circles, $5 \times 10^4 \text{ s}^{-1}$; solid circles, $3.76 \times 10^5 \text{ s}^{-1}$; solid triangles, $6.28 \times 10^5 \text{ s}^{-1}$; open squares, $9.42 \times 10^5 \text{ s}^{-1}$; solid squares, $1.26 \times 10^6 \text{ s}^{-1}$; open triangles, $1.88 \times 10^6 \text{ s}^{-1}$.

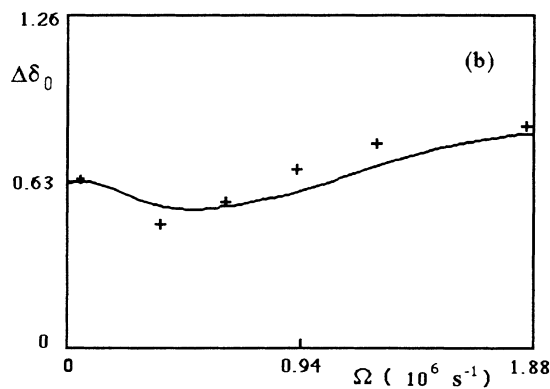
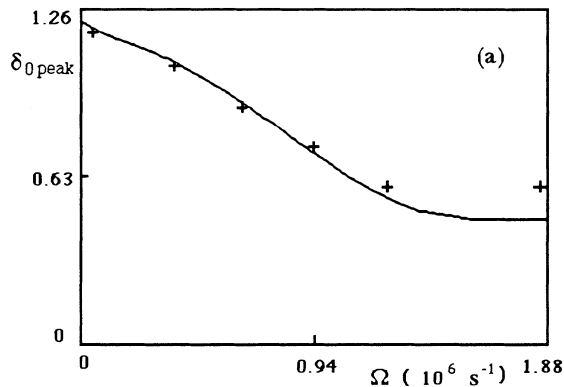


FIG. 8. Collection of experimental results for (a) value of δ_0 at the peak of $a_0(\delta_0)$ and (b) half-width at half-maximum of that curve ($\Delta\delta_0$) as functions of Ω with best fitted values of corresponding curves for the two-level model using decay rates giving $\kappa = (7.2 \pm 0.3) \times 10^6 \text{ s}^{-1}$, $\gamma_{\parallel} = (1.4 \pm 0.2) \times 10^5 \text{ s}^{-1}$ for the two-level model.

for $(J+1)\gamma_R$.

For the Lorentzian pressure-broadened linewidth γ_{\perp} of the transition, we refer to the empirical formula of Judd, quoted by Smith, DuGuay, and Ippen and also by Degnan,²⁹ which takes the following form for gas temperatures of order 300 K:

$$(2.38P_{\text{CO}_2} + 1.74P_{\text{N}_2} + 1.43P_{\text{He}}) \times 10^7 \text{ s}^{-1} \text{ Torr}^{-1},$$

which for our pressure mixture gives $2.55 \times 10^8 \text{ s}^{-1}$. The total linewidth is a convolution of the homogeneously broadened lineshape with a Gaussian Doppler-broadened linewidth of $1.67 \times 10^8 \text{ s}^{-1}$ (53 MHz full width), which

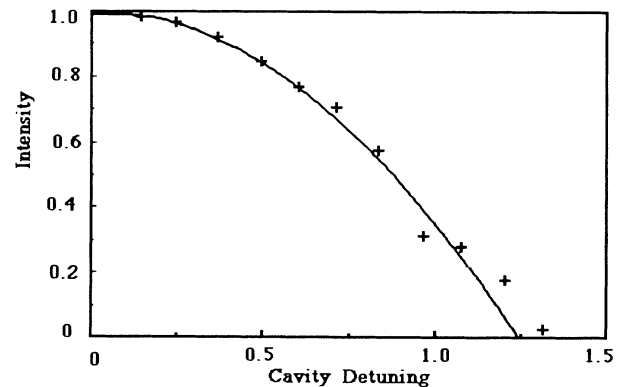


FIG. 9. Plot of I_{SS} vs cavity detuning for experimental data. Intensities are normalized to unity at zero detuning. Cavity detuning is measured in units of γ_{\perp} .

we estimate to reach about $3.05 \times 10^8 \text{ s}^{-1}$. (Note that all decay rates, and hence also linewidths, are in radians per second and correspond to half-widths at half-maximum of the spectral line shapes.)

For the population decay rates for these partial pressures, the empirical formula of Cheo for the decay of the bottleneck level in the decay channel of the lower lasing level²²

$$[(1.94 \times 10^2)P_{\text{CO}_2} + (6.5 \times 10^4)P_{\text{H}_2} + (6.5 \times 10^2)P_{\text{N}_2} + (3.27 \times 10^3)P_{\text{He}}] \text{s}^{-1} \text{Torr}^{-1}$$

gives a value for γ_{\parallel} at our pressures of $4.2 \times 10^4 \text{ s}^{-1}$. Independent measurements of the effective decay rate of the lower lasing level [Table 15 in Ref. 22 (p. 161)] gives an empirical formula

$$[2.2P_{\text{CO}_2} + 33P_{\text{H}_2} + 0.026P_{\text{N}_2} + 4.7P_{\text{He}} + 5P_{\text{Xe}} + (1.2 \times 10^3)P_{\text{H}_2\text{O}}] \times 10^3 \text{s}^{-1} \text{Torr}^{-1},$$

which yields a value for γ_{\parallel} at our pressures of $6.5 \times 10^4 \text{ s}^{-1}$, which we can safely assume is accurate to about 20%. In the effective two-level model for CO_2 lasers this decay rate becomes the γ_{\parallel} . [Alternative formulas for the population decay rates can be derived from Table II in Ref. 30 (p. 146) and Table 3.4 in Ref. 21 (p. 76) yielding values of order $5 \times 10^2 \text{ s}^{-1} \text{Torr}^{-1}$.]

(Note that the bottleneck value is about an order of magnitude larger than the values found in Refs. 21 and 29 and that quoted in Refs. 5, 19, 24, and 25 where $5 \times 10^3 \text{ s}^{-1}$ is used for lasers operating at 10 Torr, consistent with the measurement of Ref. 29 at 1 Torr CO_2 . In contrast $5 \times 10^4 \text{ s}^{-1}$ at 10 Torr is more consistent with the measurements reported by Cheo. (The confusion over the use of $5 \times 10^3 \text{ s}^{-1}$ at 10 Torr for the population decay rate arises from considerations that appear in Ref. 31, which reports a lifetime of $[5 + 3.7P(\text{Torr})] \times 10^2 \text{ s}^{-1}$ for the lifetime of the upper vibrational band 00⁰1, and from concerns about getting the correct output powers for CO_2 lasers from the rate equations where the saturation intensity is fixed by the rate constants.) If the lower value is correct, then the bottleneck is not the limiting constraint.)

In any case, the authors of Refs. 19 and 25 demonstrate that an artificially increased value of $5 \times 10^5 \text{ s}^{-1}$ is required to find agreement between their swept or switched gain experiments and the two-level model. Hence they chose to use the vibro-rotational model instead. Similarly, the authors of Ref. 17 who quote the value from Cheo as the "true" characteristic of CO_2 find that they must also use a value of order $3 \times 10^5 \text{ s}^{-1}$ for the decay of the lower lasing level to obtain agreement between their experimental results at 18 Torr and theoretical results from their three-level model of the transitions in the CO_2 gain medium of a laser with a saturable absorber.

Clearly confusion reigns—a confusion which we hope to resolve somewhat (at least for dynamics) from our measured results. However, we will have to approximate the partially inhomogeneously broadened medium by pa-

rameters that we can use in models that assume homogeneous broadening. It is worth noting that studies of the stability of inhomogeneously broadened single-mode lasers with a two-level medium have been done³² and the methods of those studies could be used to find the corrections to the eigenvalues in at least that simple case, though the amount of computational difficulty in such procedures and the doubtful exactness of the results leads us simply to refer to that possibility.

ANALYSIS OF RESULTS

To complete this analysis on the assumption of homogeneous broadening we need to adopt a value of γ_{\perp} to use in the normalization of the detuning parameter δ and for determination of the value of the pump parameter. We also need to adopt a value of $(J+1)\gamma_R$ to use in the more complicated formulas for the vibrational-rotational model. Conventional wisdom is that the same processes are involved and thus that the values should be the same. One might conclude from the literature cited above that the values are known with poor precision and that the rotational and collision decay rates might differ by as much as a factor of 2. We choose the values $2.55 \times 10^8 \text{ s}^{-1}$ for both, which must be assigned uncertainties in the range of 20% given the uncertainties implicit in the formulas and the additional errors induced by the inhomogeneous broadening.

From the maximum cavity detuning range (of the fundamental longitudinal mode) as a fraction of one-half of the free spectral range measured directly as 0.83 ± 0.02 and from the mode pulling factor given by $\kappa/\gamma_{\perp} = 0.067$ we determined the value of A (using $I = A - 1 - \delta^2$) in our experiments to be 2.6 ± 0.5 .

From Fig. 8 and the fitting procedure we extract the values of $\omega_{0_{\text{max}}}$ and β_{max} as follows:

$$\omega_{0_{\text{max}}} = (1.74 \pm 0.28) \times 10^6 \text{ rad/sec},$$

$$\beta_{\text{max}} = (3.8 \pm 0.8) \times 10^5 \text{ s}^{-1}.$$

Note that the value of β_{max} is comparable to the value of $\omega_{0_{\text{max}}}$ and unusually large if it is equal to $A\gamma_{\parallel}$ given the population decay rate of a CO_2 laser if it is described by a two-level model; however, it is consistent with the relatively few oscillations in transients observed in some recent experiments.¹⁹

The estimates for the γ 's permit us to compare in Table I the values of κ and γ_{\parallel} from these independent determinations with those measured from the experiment using the relations for the two-level model and for the interband relaxation model that give the values in terms of the measured values of β_{max} and $\omega_{0_{\text{max}}}$.

We see that the agreement between the measured values and the known parameters of the laser we used and the properties of the CO_2 medium is better for the vibro-rotational model with about 25 ± 5 coupled levels. This is consistent the value of 16 reported in Refs. 19 and 25 for the P20 line. Further refinements in the fitting procedure may give even more accurate estimates. Independent measurements of the cavity-loss rate instead of

TABLE I. Comparison of values of γ_{\parallel} and κ from estimates and models. Using $A=2.6$, $\gamma_{\perp}=2.55 \times 10^7 \text{ s}^{-1}$ and the measured values of β_{\max} and $\omega_{0_{\max}}$ we can also calculate the relaxation rates for the different models.

	$\gamma_{\parallel} \text{ (s}^{-1}\text{)}$	$\kappa \text{ (s}^{-1}\text{)}$
Estimated from experiment	$(6.5 \pm 1.3) \times 10^4$	$(1.7 \pm 0.3) \times 10^7$
Two-level model	$(1.4 \pm 0.2) \times 10^5$	$(7.2 \pm 0.3) \times 10^6$
Vibrational-rotational model		
$J=5$	$(1.2 \pm 0.1) \times 10^5$	$(0.81 \pm 0.01) \times 10^7$
$J=10$	$(1.1 \pm 0.2) \times 10^5$	$(0.90 \pm 0.08) \times 10^7$
$J=20$	$(8.4 \pm 0.8) \times 10^4$	$(1.20 \pm 0.50) \times 10^7$
$J=30$	$(6.3 \pm 0.8) \times 10^4$	$(1.60 \pm 0.70) \times 10^7$

estimates thereof would permit more exact determination by self-consistency of the values of J and γ_R in the vibro-rotational model and measurements on different lines of a CO₂ laser could determine the number of levels involved in the intraband couplings as a function of the position of the level in the band. We see, for example, that if one used the lower value for γ_R given by Cheo, then we would obtain a larger value of κ and a smaller value of γ_{\parallel} which would fit the data even better. Perhaps these discrepancies could be used to test the assumption that $(J+1)\gamma_R$ is equal to γ_{\perp} or to test the assumption of the validity of this vibrational-rotational model.

FINAL DISCUSSION

In summary, we should note that the careful study of the behavior of the linear response of a cavity-modulated class-B laser as the laser is detuned provides a sensitive measure of the properties of the intrinsic damped oscillator (the relaxation oscillations) that underlies the approach to stable laser operation. Although there is no response for resonant tuning of the laser cavity, the sensitivity of the amplitude of the linear response to the value of detuning suggests that studies of more complex nonlinear dynamics of modulated lasers need careful control of the values of the parameters.

It is not surprising that any system with a damped relaxation oscillation can be described by an effective simple damped oscillator equation. The formal justification for this is provided by the center-manifold theory. What is clear is that the simple two-level atom model is too constrained to describe the behavior of the CO₂ laser when one uses physically realistic parameters. It is likely that many more complicated models will have sufficiently many degrees of freedom in their parameters that a more realistic effective oscillator on the slow manifold can be found. However, the vibrational-rotational model seems to be a particularly attractive candidate model because of its physical basis and the tractability of its analysis using center-manifold techniques as demonstrated in Ref. 24.

ACKNOWLEDGMENTS

This work was supported in part by a grant from the National Natural Science Foundation of China and began as a follow-up to a lecture series presented under the sponsorship of the Optical Society of America. We are grateful for helpful discussions with E. Arimondo, D. Dangoisse, P. Glorieux, D. Hennequin, G. L. Oppo, and J. R. Tredicce. Laboratoire de Spectroscopie Hertzienne is associ   au Centre National de la Recherche Scientifique.

*Permanent address: Department of Physics, Bryn Mawr College, Bryn Mawr, PA 19010-2899.

¹R. W. Hellwarth, Phys. Rev. Lett. **6**, 9 (1961); in *Advances in Quantum Electronics*, edited by J. R. Singer (Columbia University Press, New York, 1961), p. 334; N. G. Basov, V. S. Zuev, P. G. Krjukiv, in *Lasers*, edited by J. Weber (Gordon Breach, New York, 1968), Vol. XA, p. 257.

²For a specific discussion of distortions during intracavity loss modulation of a CO₂ laser see A. Yariv, T. A. Nussmeier, and J. E. Kieffer, IEEE J. Quantum Electron. **QE-9**, 594 (1973). For detailed references and a review, see sections on relaxation oscillations and on modulated parameters in N. B. Abraham, P. Mandel, and L. M. Narducci, in *Progress in Optics*, edited by E. Wolf (Elsevier, Amsterdam, 1978), Vol. XXV, p. 1; L. M. Narducci and N. B. Abraham, *Laser Physics and Laser Dynamics* (World Scientific, Singapore, 1988); for a cor-

respondingly comprehensive review restricted only to modulated parameters (in Russian) see A. M. Samson and S. I. Turovets, Dokl. Akad. Nauk SSSR **31**, 888 (1987); Zh. Prikl. Spektrosk. **48**, 384 (1988).

³(a) The classifications based on different relaxation rates were effectively explored when the dynamics of the three variables in turn were adiabatically eliminated by studies by C. L. Tang, J. Appl. Phys. **34**, 2935 (1963); (b) E. M. Belenov, V. N. Morozov, and A. N. Oraevsky, in *Quantum Electronics of Masers and Lasers*, edited by D. V. Skobel'tsyn (Plenum, New York, 1972), Part 2, p. 217; V. N. Genkin and Ya. I. Khanin, Izv. Vyssh. Uchebn. Zaved. Radiofiz. **3**, 423 (1962).

⁴(a) J. R. Tredicce, F. T. Arecchi, G. L. Lippi, and G. P. Puccioni, J. Opt. Soc. Am. **B 2**, 173 (1985); see also (b) F. T. Arecchi, in *Optical Instabilities*, edited by R. W. Boyd, M. G. Raymer, and L. M. Narducci (Cambridge University Press, Cam-

- bridge, 1986), p. 183; (c) F. T. Arecchi, in *Instabilities and Chaos in Quantum Optics*, edited by F. T. Arecchi and R. W. Harrison (Springer-Verlag, Berlin, 1987), p. 9.
- ⁵F. T. Arecchi, R. Meucci, G. P. Puccioni, and J. R. Tredicce, *Phys. Rev. Lett.* **49**, 1217 (1982).
- ⁶O. R. Wood and S. E. Schwartz, *Appl. Phys. Lett.* **11**, 88 (1967); G. P. Puccioni, A. Poggi, W. Gadomski, J. R. Tredicce, and F. T. Arecchi, *Phys. Rev. Lett.* **55**, 339 (1985); J. R. Tredicce, F. T. Arecchi, G. P. Puccioni, A. Poggi, and W. Gadomski, *Phys. Rev. A* **34**, 2073 (1986); A. Poggi, G. P. Puccioni, W. Gadomski, F. T. Arecchi, and J. R. Tredicce, in Ref. 4(b), p. 303; see also Ref. 4(b); L. X. Chen, A.-Q. Ma, and C.-F. Li, *Opt. Sinica* **8**, 132 (1988).
- ⁷J. R. Tredicce, N. B. Abraham, G. P. Puccioni, and F. T. Arecchi, *Opt. Commun.* **55**, 131 (1985).
- ⁸D. J. Biswas, V. Dev, and U. K. Chatterjee, *Phys. Rev. A* **35**, 456 (1987).
- ⁹T. Midavaine, D. Dangoisse, and P. Glorieux, *Phys. Rev. Lett.* **55**, 1989 (1985); D. Dangoisse, P. Glorieux, and D. Hennequin, *ibid.* **57**, 2657 (1986); *Phys. Rev. A* **36**, 4775 (1987); F. Papoff, D. Dangoisse, E. Poite-Hanoteau, and P. Glorieux, *Opt. Commun.* **67**, 358 (1988); D. Dangoisse, P. Glorieux, and D. Hennequin, *Phys. Rev. A* **36**, 4775 (1987).
- ¹⁰K. Gurs, in *Quantum Electronics*, edited by P. Grivet and N. Bloembergen (Dunod, Paris, 1964), p. 1113; C. L. Tang, H. Statz, and G. Demars, *Appl. Phys. Lett.* **2**, 222 (1963); more recently, see P. A. Khandokhin and Ya. I. Khanin, *Kvantovaya Elektron. (Moscow)* **11**, 1483 (1984) [*Sov. J. Quantum Electron.* **14**, 1004 (1984)]; W. Klische, H. R. Telle, and C. O. Weiss, *Opt. Lett.* **9**, 561 (1984); E. Brun, B. Derighetti, P. Meier, R. Holzner, and M. Ravani, *J. Opt. Soc. Am. B* **2**, 156 (1985); M. W. Phillips, H. Gong, A. I. Ferguson, and D. C. Hanna, *Opt. Commun.* **61**, 215 (1987); D. C. Hanna, R. G. Smart, P. J. Suni, A. I. Ferguson, and M. W. Phillips, *ibid.* **68**, 129 (1988); K. Kubodera and K. Otsuka, *IEEE J. Quantum Electron.* **QE-17**, 1139 (1981).
- ¹¹I. I. Matorin, H. S. Pikovskii, and Ya. I. Khanin, *Kvantovaya Elektron. (Moscow)* **11**, 2096 (1984); T. Erneux, S. M. Baer, and P. Mandel, *Phys. Rev. A* **35**, 1165 (1987); P. Mandel, P. Nardone, and T. Erneux, *J. Opt. Soc. Am. B* **5**, 1113 (1988).
- ¹²M. James and F. Moss, *J. Opt. Soc. Am. B* **5**, 1121 (1988).
- ¹³R. Meucci, A. Poggi, F. T. Arecchi, and J. R. Tredicce, *Opt. Commun.* **65**, 131 (1988); H. G. Solari, E. Eschenazi, R. Gilmore, and J. R. Tredicce, *ibid.* **64**, 49 (1987).
- ¹⁴B. K. Goswami and D. J. Biswas, *Phys. Rev. A* **36**, 975 (1987).
- ¹⁵E. Arimondo, F. Casagrande, L. A. Lugiato, and P. Glorieux, *Appl. Phys. B* **30**, 57 (1983); M. L. Asquini and F. Casagrande, *Nuovo Cimento* **2D**, 917 (1984).
- ¹⁶G. L. Oppo and A. Politi, *Z. Phys. B* **59**, 111 (1985); *Europhys. Lett.* **1**, 549 (1986).
- ¹⁷M. Tachikawa, K. Tanii, M. Kajita, and T. Shimizu, *Appl. Phys. B* **39**, 83 (1986); M. Tachikawa, K. Tanii, and T. Shimizu, *J. Opt. Soc. Am. B* **4**, 387 (1987); M. Tachikawa, F.-L. Hong, K. Tanii, and T. Shimizu, *Phys. Rev. Lett.* **60**, 2266 (1988).
- ¹⁸B. Zambon, F. DeTomasi, D. Hennequin, and E. Arimondo, in *Technical Digest, International Workshop on Instabilities, Dynamics and Chaos in Nonlinear Optical Systems*, edited by N. B. Abraham, E. Arimondo, and R. W. Boyd (ETS Editrice, Pisa, 1987); F. DeTomasi, D. Hennequin, B. Zambon, and E. Arimondo, *J. Opt. Soc. Am. B* **6**, 45 (1989); B. Zambon, F. DeTomasi, D. Hennequin, and E. Arimondo, *Phys. Rev. A* **40**, 3782 (1989). [See also a simplified model obtained by partial adiabatic elimination D. Dangoisse and P. Glorieux, *J. Opt. Soc. Am. B* (to be published).]
- ¹⁹F. T. Arecchi, W. Gadomski, R. Meucci, and J. A. Roversi, *Opt. Commun.* **65**, 47 (1988); **70**, 155 (1989); see also F. T. Arecchi, W. Gadomski, R. Meucci, and J. A. Roversi, in *Optical Bistability IV*, edited by W. Firth, N. Peyghambarian, and A. Tallet (Les Editions de Physique, Paris, 1988), p. C2-363.
- ²⁰I. Burak, P. L. Huston, D. G. Sutton, and J. I. Steinfeld, *IEEE J. Quantum Electron.* **QE-7**, 73 (1971); J. Dupré, F. Meyer, and C. Meyer, *Phys. Rev. Appl. (Paris)* **10**, 285 (1975).
- ²¹E. J. Witteman, *CO₂ Lasers* (Springer, Berlin, 1987).
- ²²P. K. Cheo, in *Lasers 3*, edited by A. Levine (Dekker, New York, 1971), p. 111 (for the details of the pressure broadening rates see p. 154).
- ²³R. A. Rooth, J. A. Van Der Pol, E. H. Haselhoff, and W. J. Witteman, *IEEE J. Quantum Electron.* **QE-23**, 1372 (1987); C. Dang, J. Reid, and B. K. Garside, *Appl. Phys. B* **27**, 145 (1982); **31**, 163 (1983); *IEEE J. Quantum Electron.* **QE-19**, 755 (1983).
- ²⁴G. L. Oppo, J. R. Tredicce, and L. M. Narducci, *Opt. Commun.* **69**, 393 (1989).
- ²⁵F. T. Arecchi, R. Meucci, and J. A. Roversi, *Europhys. Lett.* **8**, 225 (1989); F. T. Arecchi, W. Gadomski, R. Meucci, and J. A. Roversi, *Phys. Rev. A* **39**, 4004 (1989).
- ²⁶G. L. Oppo and A. Politi, *Phys. Rev. A* **40**, 1422 (1989).
- ²⁷W. L. Nighan, *Phys. Rev. A* **2**, 1989 (1970).
- ²⁸K. R. Manes and H. J. Seguin, *J. Appl. Phys.* **43**, 5073 (1972).
- ²⁹P. W. Smith, M. A. Duguay, and E. P. Ippen, *Prog. Quantum Electron.* **3**, 105 (1974), see p. 158; J. J. Degnan, *Appl. Phys.* **11**, 1 (1976), see p. 26.
- ³⁰D. C. Tyte, in *Advances in Quantum Electronics*, edited by D. W. Goodwin (Academic, New York, 1970), pp. 129–198.
- ³¹L. O. Hocker, M. A. Kovacs, C. K. Rhodes, G. W. Flynn, and A. Javan, *Phys. Rev. Lett.* **17**, 233 (1966).
- ³²N. B. Abraham, L. A. Lugiato, P. Mandel, L. M. Narducci, and D. K. Bandy, *J. Opt. Soc. Am. B* **2**, 35 (1985); D. K. Bandy, L. M. Narducci, L. A. Lugiato, and N. B. Abraham, *ibid.* **2**, 56 (1985).